J. Ocean Univ. China (Oceanic and Coastal Sea Research)
https://doi.org/10.1007/s11802-023-5478-8
ISSN 1672-5182, 2023 22 (4): 1087-1097
http://www.ouc.edu.cn/xbywb/
E-mail:xbywb@ouc.edu.cn

Transcriptome Analysis of Mantle Tissues Reveals Potential Shell-Matrix-Protein Genes in *Gigantidas haimaensis*

SHI Yu[1), 2)], YAO Gaoyou[1), 3)], and HE Maoxian[1), 2), *]

1) *CAS Key Laboratory of Tropical Marine Bio-Resources and Ecology*, *Guangdong Provincial Key Laboratory of Applied Marine Biology*, *South China Sea Institute of Oceanology*, *Chinese Academy of Sciences*, *Guangzhou* 510301, *China*
2) *Southern Marine Science and Engineering Guangdong Laboratory (Guangzhou)*, *Guangzhou* 511458, *China*
3) *University of Chinese Academy of Sciences*, *Beijing* 100049, *China*

(Received June 14, 2022; revised September 19, 2022; accepted November 25, 2022)

Abstract *Haima* cold seep ecosystem is on the northwestern slope of the South China Sea, which is characterised by high pressure, low temperature, hypoxia, and low pH value. The deep-sea mussel *Gigantidas haimaensis* is distributed in this ecosystem. Previous studies have focused on its adaptation to abiotic stress, biogeography, ecotoxicology, genomes, immunity and symbiosis, but knowledge on biomineralisation remains lacking. Herein, we generated a comprehensive transcript dataset from *G. haimaensis* mantle tissue, and 30255 unigenes were assembled. The top 20 most highly expressed genes are related to energy supply, such as mitochondrial genes, suggesting they may mediate the adaptability of this deep-sea mussel to the high pressure and hypoxia environment. Eleven shell matrix protein (SMP)-related genes were identified from the transcriptome data. Quantitative PCR analyses showed that five of ten acidic SMPs and nacreous-layer-matrix-protein genes (*nacrein*, *perlucin*, *perlwapin*, *pif* and *mantle protein*) were highly expressed in mantle tissue, while the expressions of other five genes (*chitinase*, *SPARC*, *TRY*, *papilin* and *calmodulin*) were low. Scanning electron microscopy showed that the shell was composed of a prismatic layer and a nacreous layer, and every nacreous layer was made of the whole pieces of aragonite that stacked on top of each other. These results indicated the conservation of the structure and functions of nacreous matrix genes in *G. haimaensis*. Moreover, the nacreous layer was made of whole pieces of aragonite that were not quadrilateral or polygonal pieces. Studying these genes will likely reveal the molecular mechanisms of biomineralisation in *G. haimaensis* and other deep-sea mussels.

Key words *Gigantidas haimaensis*; transcriptome; biomineralisation; mantle; shell structure

1 Introduction

In many species from prokaryotes to eukaryotes, biomineralisation is a crucial process that usually occurs with ontogeny. Bacterial magnetosomes, sea urchin spicules, shells, animal teeth and bones are all products of mineralisation. Biological minerals are mainly composed of inorganic substances that endow organisms with the ability to forage, navigate and defend themselves (Semeao *et al*., 1999).

One of the most interesting issues in biological mineralisation is the molecular mechanism that regulates the deposition of inorganic ions into the solid phase in certain order. Studies have shown that organic matter is mainly composed of chitin, proteins and other organic macromolecules that account for <5% of the total weight of living minerals, but it may play a pivotal role in the regulation of mineralisation (Heuer *et al*., 1992). Previous studies show that these organic components play an important regulatory role in controlling the nucleation, arrangement and growth of calcium carbonate crystals and the development and formation of shells (Dujardin and Mann, 2002). Therefore, elucidating the functions of shell matrix proteins (SMPs) is a major goal of biological mineralisation research (Huang *et al*., 2003).

SMPs are considered the key factors regulating the formation of these structures, hence it is very important to study the mechanisms and functions of SMPs to understand the mechanism of shell mineralisation. Important SMPs have been studied using biochemical isolation and purification, amino acid sequencing, molecular cloning and omics approaches. These studies revealed that MSI60 (Sudo *et al*., 1997), N19 (Wang *et al*., 2009), Pearlin/N16 (Miyashita *et al*., 2000), PNU9 (Kong *et al*., 2019), Pif (Abe *et al*., 2007; Suzuki *et al*., 2009) and other proteins all play a pivotal role in the formation of the nacreous layer. Meanwhile, MSI7 (Zhang *et al*., 2003), KRMP family members (Masaoka and Kobayashi, 2009), Prismalin-14 (Suzuki *et al*., 2004), Prisilkin-39 (Kong *et al*., 2009), Mpn88 (Mariom *et al*., 2019), and other proteins play a key role in the formation of the prismatic layer. These studies have laid a solid foundation for investigating the shellfish biomineralisation mechanism through analysing the structural and functional of matrix

* Corresponding author. E-mail: hmx2@scsio.ac.cn

proteins.

Since the advent of second-generation sequencing technologies, research on the mechanism of shell biomineralisation can be carried out using omics approaches with high speed and accuracy, which can also generate large quantities of sequence data. Transcriptome sequencing has been performed on mantle tissues of various shellfish, revealing genes involved in shell formation including lectins, shematrins, lysine-rich SMPs (KPMPs), mantle genes, met-rich matrix, secreting calcium-binding proteins, proteases, protease inhibitors, glycine-rich shell SMPs, calponin-like protein, calcineurin-binding protein, follistatin-like and carbonic anhydrase 1, and others (Shi *et al*., 2013a, 2013b; Werner *et al*., 2013; Artigaud *et al*., 2014; Deng *et al*., 2014; Freer *et al*., 2014).

One group identified 80 SMPs from the prismatic and nacreous layers of the shell of *Pinctada margaritifera* and *Pinctada maxima* (Marie *et al*., 2012). MSP130, IPC-1, superoxide dismutase and even cytoskeleton actin proteins were found in the shell *Laqueus rubellus*, suggesting there may be some similarity in the mechanisms of extracellular and intracellular crystallisation (Isowa *et al*., 2015). Shell SMPs contain not only functional proteins related to conserved mineralisation processes, but also proteins encoded by germline-specific genes that often share high amino acid sequence identity, reflecting homology and differences in biological mineralisation during evolution.

SMPs can be classified according to their physical and chemical properties, and amino acid characteristics, as well as the distribution and isoelectric point differences of SMPs in different mineralised structures of shells. Using this approach, SMPs can be divided into acidic and alkaline SMPs.

1) Acidicic SMP: Major acidic SMPs include MSP-1 (Sarashina and Endo, 2001), MSP-2 (Hasegawa and Uchiyama, 2005), PfN44 (Pan *et al*., 2014), Mpn88 (Mariom *et al*., 2019) and others. One characteristic of acidic SMPs is an isoelectric point (pI)<6. These proteins are more abundant in the prismatic layer, and they promote calcite crystallisation *in vitro* (Ren *et al*., 2011). Some acidic SMPs are found in the nacreous layer, including Nacrein (Miyamoto *et al*., 1996), Pearlin/N16 (Miyashita *et al*., 2000), Pif (Suzuki *et al*., 2009) and others. Additionally, there are some extrapallial fluid proteins such as ACCBP (Ma *et al*., 2007) and SPARC (Miyamoto *et al*., 2013).

2) Alkaline SMP: A few alkaline SMPs are extremely alkaline, including some members of the KRMP protein family (Masaoka and Kobayashi, 2009), PNU9 (Kong *et al*., 2019), and others. Others are weakly alkaline, such as Shematrin family proteins (Yano *et al*., 2006) and others. Additionally, there are some extrapallial fluid proteins including PFMG1 (Liu *et al*., 2007) and EFCBP (Huang *et al*., 2007).

3) Shell frame protein: According to the solubility of SMPs during the extraction process, they can be divided into EDTA-soluble and EDTA-insoluble proteins, among which shell frame proteins constitute the main components of insoluble SMPs. As an organic support of shells, frame proteins participate in the construction of mineralised structures. Main frame proteins include KRMP family proteins (Masaoka and Kobayashi, 2009), Shematrin family proteins (Yano *et al*., 2006) and others.

Much of our current understanding of biomineralisation is derived from shallow marine species, which limit our understanding about the diversity of biomineralisation. Studies on biomineralisation of deep-sea molluscs is currently restricted to scaly-foot snail (*Chrysomallon squamiferum*), which revealed the biomineralised armour of lophotrochozoan lineages (Sun *et al*., 2020).

Deep-sea hydrothermal vent and seep environments are characterized by high pressure, low temperature, hypoxia, low pH values, and dense populations of invertebrates (Campbell, 2000; Levin, 2005). Among the large deep-sea fauna, deep-sea mussels *Bathymodiolus* (Bivalvia, *Mytilidae*) are widely distributed at many hydrothermal vent and cold seep ecosystems around the world (Sibuet and Olu, 1998; Campbell, 2000). Previous studies have focused on adaptation to symbiosis (Dubilier *et al*., 2008), abiotic stress (Boutet *et al*., 2009), immunity (Bettencourt *et al*., 2010), biogeography (Johnson *et al*., 2013), ecotoxicology (Bougerol *et al*., 2015) and genomes (Sun *et al*., 2017). The deep-sea mussel *Gigantidas haimaensis* is widely distributed in the *Haima* cold seep ecosystem on the northwestern slope of the South China Sea (Xu *et al*., 2019b), but limited information is available on this species.

2 Materials and Methods

2.1 Animals and Collection

G. haimaensis mantles (Fig.1) were obtained from the Haima cold seep (16.73˚N, 110.475˚E, depth 1446 m) using the manned submersible ROV Haima during cruise HYDZ6-202005 onboard the research vessel (R/V) *Haiyang 6* of the Guangzhou Marine Geological Survey (China; September 1–6, 2020). Foot, muscle, gill, mantle tissues

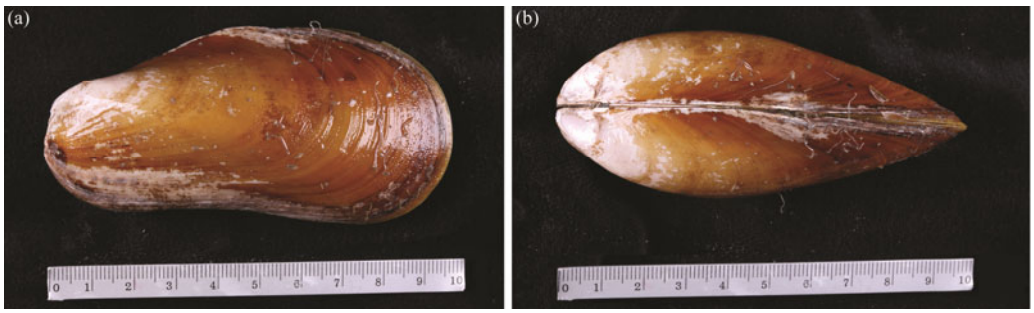

Fig.1 Photo of *G. haimaensis*. (a), Lateral view; (b), ventral view. Scale bar = 1 cm.

and digestive gland were removed from each individual, immediately frozen in liquid nitrogen for 24 h, and were then stored at −80℃. After the cruise, the samples were placed on dry ice and were transported to the South China Sea Institute of Oceanology, Chinese Academy of Sciences. All animal experiments were conducted in accordance with the guidelines and approval of the Animal Research and Ethics Committees of the Chinese Academy of Sciences.

2.2 Construction of a Complementary DNA Library and Illumina Sequencing

Total RNA was isolated from the mantle tissues of three *G. haimaensis* individuals which were used as input material to prepare the RNA sample. Construction of the complementary DNA Library and Illumina sequencing were performed as described by Shi *et al*. (2022).

2.3 Data Filtering and *de novo* Assembly

Raw data were filtered to obtain clean data and transcriptomes were separately assembled *de novo* following the methods reported by Shi *et al*. (2022).

2.4 Gene Functional Annotation

Based on the study of Shi *et al*. (2022), gene functions were annotated using the following databases: Nr (NCBI non-redundant protein sequences), Nt (NCBI non-redundant nucleotide sequences), Pfam (Protein family), KOG/COG (Clusters of Orthologous Groups of proteins), Swiss-Prot (manually annotated and reviewed protein sequence), KO (KEGG Ortholog database) (Mao *et al*., 2005) and GO (Gene Ontology) databases (Young *et al*., 2010).

2.5 Quantitative Real-Time PCR (qPCR) Validation

SMPs with known functions were identified. Totally 11 SMPs were found in the mantle transcriptome of *G. haimaensis*, and all were subjected to qPCR validation. Foot, muscle, gill, mantle, and digestive gland (DG) tissues of *G. haimaensis* were collected from three mussels for qPCR, following the protocol described by Shi *et al*. (2022) using primers listed in Table 1, with 60S ribosomal protein L15 (*60S RP-L15*) as a reference gene.

2.6 Scanning Electron Microscopy (SEM) Images of the *G. haimaensis* Shell

The shell of each individual was thoroughly cleaned with Milli-Q water and then air-dried. Subsequently, the shells were broken into sheets and were fixed on the scanner with the inner nacreous surface pointing upward. Then they were sputter-coated with 10-nm-thick gold and analyzed using SEM (S-3400N; Hitachi, Japan).

Table 1 List of primers for quantitative PCR analyses

Gene name	Tran ID	Primer sequence (5'→3')
chitinase	Cluster-1047.0	F: AACAACAGCACAACCCAC R: AGTTCGCATTACATTTCC
ferritin	Cluster-6061.5082	F: CAAAGTCAACCTCGTCAA R: GAATCCTGGGAGTGCTAC
nacrein	Cluster-185.0	F: CACCCTAATTCTCGTTCA R: ACGGTGGAGACATGGTAC
perlucin	Cluster-6061.5440	F: TCAGTCAATGGGCTCCTA R: ATTTCAGCACAAGTTTCG
pelwapin	Cluster-18936.0	F: TCTTAGCCAATCACAATG R: CACAACCAGAGGGACAAC
pif	Cluster-13568.0	F: TAAAGAACGGAACGGAGAC R: TGTAACGAACACCGAAGG
SPARC	Cluster-9682.0	F: GATTGGGTCCTCGTCGTCTT R: ATCGGCTGCTTTACCACTTC
TRY	Cluster-4548.0	F: ATGGGCGAAGATTGGAGA R: GCAGCAGCACATTGGTTG
60S RP-L15	Cluster-4389.7866	F: AGCATCTGACACGGAGCA R: GACACGAGCCAGCAAGAA

3 Results

3.1 Sequence Analysis and *de novo* Assembly

Illumina sequencing of mantle tissue transcriptomes generated 65274446 raw reads with a length of 100 bp, which were reduced to 63108634 (96.68%) after quality filtering (Table 2). From each library, 21036211 filtered clean reads with Q20 > 97.12% and Q30 > 92.58% were obtained. The raw reads were submitted to the Science Data Bank under accession numbers CSTR 31253.11.sciencedb.01540/DOI 10.11922/sciencedb.01540. All sequencing reads are available through NCBI under bioproject accession number PRJNA823813. Reads were assembled *de novo* into 49101 transcripts, with a median contig of 596 bp and an N50 of 918 bp (Table 3). These transcripts were subsequently assembled into 30255 unigenes, with an average contig of 763 bp (Table 4). Benchmarking Universal Single-Copy Orthologs (BUSCO) revealed a transcriptome complete (single) value of 53%, indicating high-quality *de novo* assembly.

3.2 Gene Annotation

In total, 14529 (48.02%) of the 30255 unigenes were an-

Table 2 Clean data summary

Sample	Raw_reads	Clean_reads	Clean_bases	Error_rate	Q20	Q30	GC_pct
M1	21541544	20714655	6.21G	0.03	97.12	92.58	34.12
M2	20732814	20026738	6.01G	0.03	97.73	93.64	34.95
M3	23000088	22367241	6.71G	0.03	97.61	93.31	34.61

Table 3 List of frequency distribution of splicing length

Length_interval	300 bp−500 bp	500 bp−1 kbp	1 kb−2 kbp	>2 kbp	Total
Number of transcripts	19236	18614	9812	1439	49101
Number of Unigenes	11914	11313	6189	839	30255

Table 4 List of splicing length distribution

	Min_length	Mean_length	Median_length	Max_length	N50	N90	Total_nucleotides
Transcripts	301	763	596	7061	918	392	37482738
Genes	301	763	597	7061	921	392	23076306

notated in at least one of the public Nr, Nt, Pfam, KOG/COG, Swiss-Prot, GO and KEGG databases with E values $\leq 1\times10^{-5}$ (Table 5). The highest percentage of unigenes was annotated in the NR database, accounting for 32.5% of all unigenes, followed by 27.29% annotated in PFAM and GO databases, 21.25% in the Swiss-Prot database, 15.3% in the NT database, 14.83% in the KO database, and 11.64% in the KOG database (Table 5). Some of the annotations derived from multiple databases. Gene sequences from *Mizuhopecten yessoensis* matched the most unigenes (29.4%), followed by *Crassostrea gigas* (16.9%), *Crassostrea virginica* (16.6%), *Mytilus galloprovincialis* (8.9%) and *Lottia gigantea* (2.7%). Most unigenes (47%) shared 60%–80% sequence identity with annotated genes, and only 3.6% shared 95%–100% similarity (Fig.2).

Based on GO analysis, all genes were linked to 869 biological processes, 187 cellular components and 169 molecular functions, mainly related to cellular process, metabolic process, cellular anatomical entity and binding (Fig.3). Meanwhile, all genes were associated with 284 KEGG annotations, mainly associated with signal transduction, translation, transport and catabolism and endocrine system (Fig.4).

Table 5 Number of genes annotated in NR, NT, KO, Swiss_prot, PFAM, GO and KOG databases

Database	Numbers of unigenes	Percentage (%)
Annotated in NR	9834	32.50
Annotated in NT	4632	15.30
Annotated in KO	4489	14.83
Annotated in Swissprot	6431	21.25
Annotated in PFAM	8258	27.29
Annotated in GO	8258	27.29
Annotated in KOG	3522	11.64
Annotated in at least one database	14529	3.03
Annotated in all databases	918	48.02
Total unigenes	30255	100

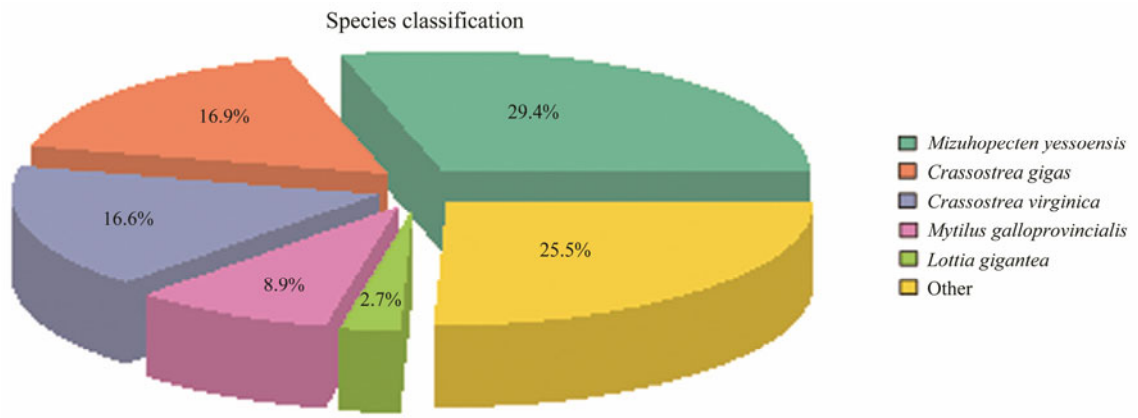

Fig.2 Species classification of sequences matching unigenes from *G. haimaensis* mantle tissue.

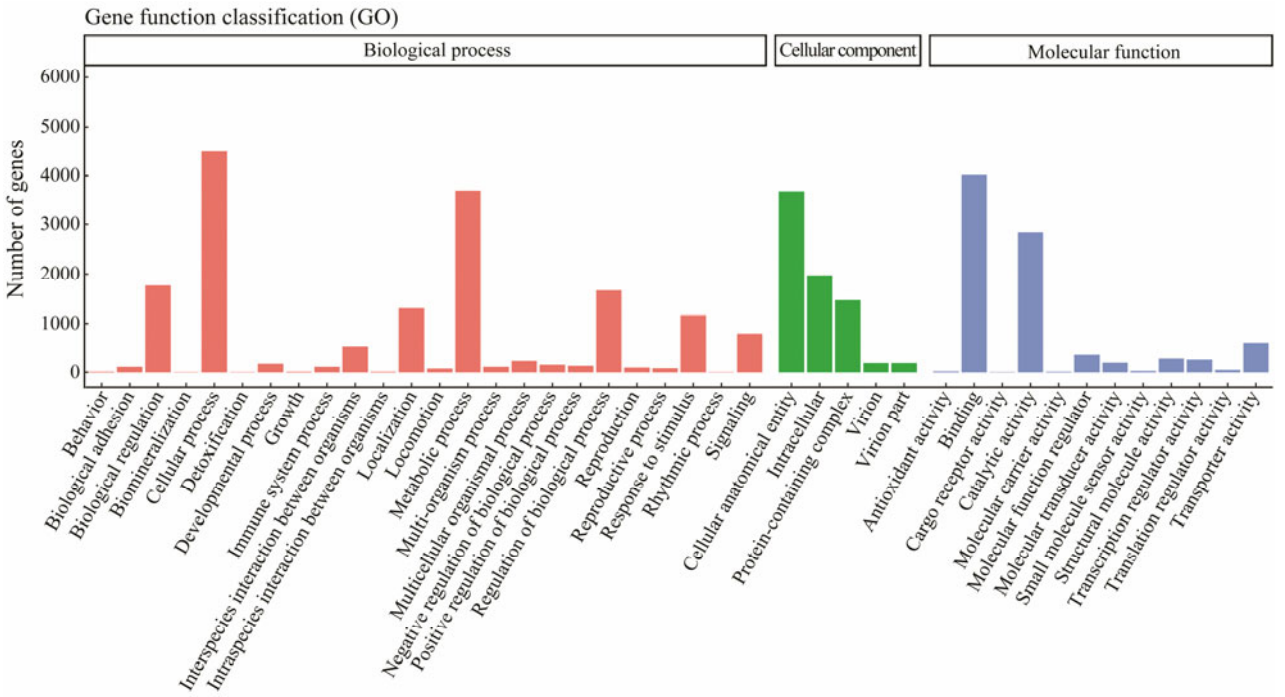

Fig.3 GO annotation classification statistics. The horizontal axis is GO terms, and the vertical axis is the number of genes annotated to GO terms.

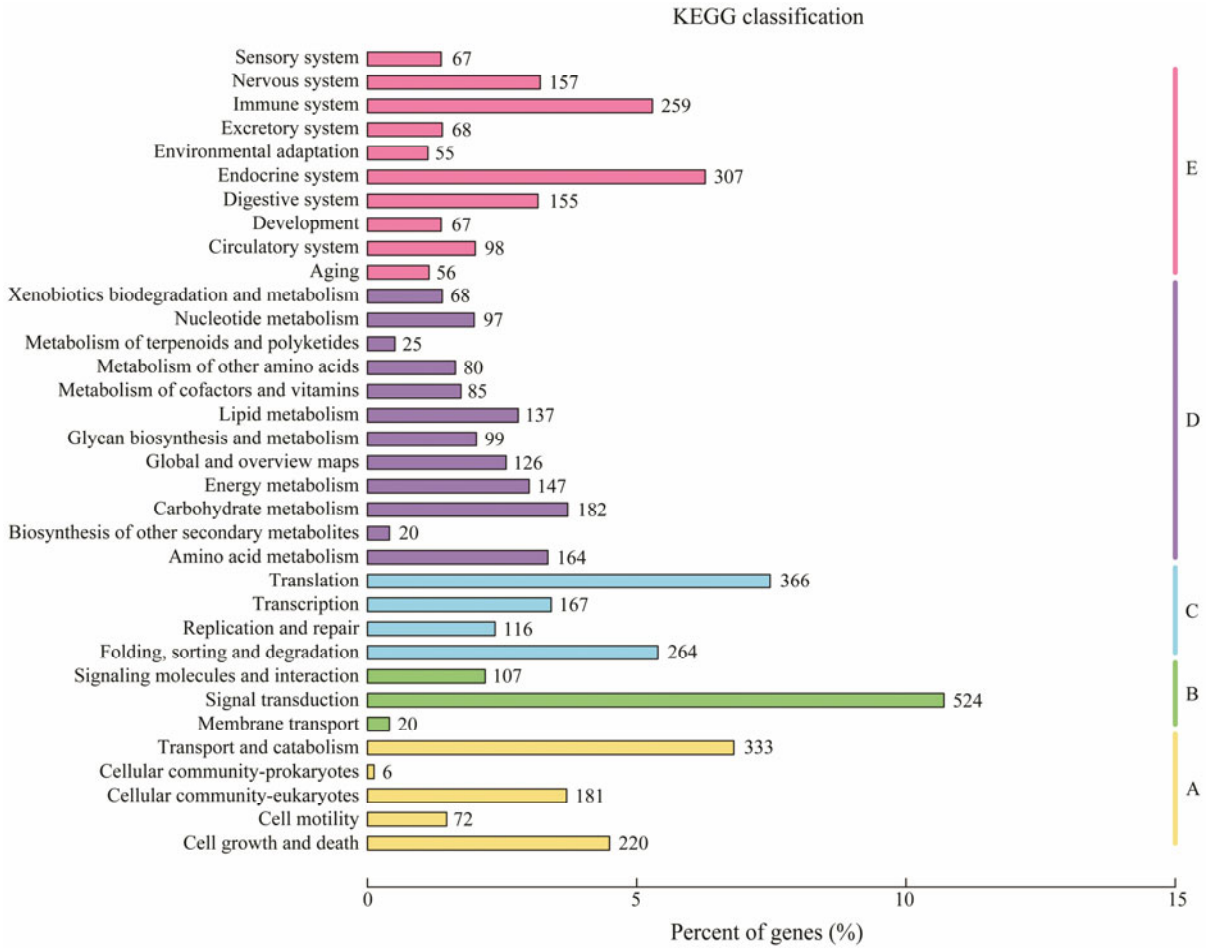

Fig.4 Statistical map of KEGG metabolic pathway classification. The vertical axis is the names of KEGG metabolic pathways, and the horizontal axis is the number of genes annotated to pathways and their proportion of the total number of genes annotated. Genes were divided into five branches according to the KEGG metabolic pathway and involved: A, cellular processes; B, environmental information processing; C, genetic information processing; D, metabolism; E, organismal systems.

3.3 Highly Expressed Genes

The top 20 genes which have the highest expression levels are listed in Table 6. The richest unique sequences were annotated as *Bathymodiolus platifrons* mitochondrion. The other highly expressed sequences included interleukin-4 receptor alpha chain, N-terminal/ATP synthase protein 8, cytochrome c oxidase subunit III (mitochondrion), ribosomal proteins and NADH dehydrogenase, as shown in Table 6.

Table 6 Most highly-expressed genes in the *Gigantidas haimaensis* transcriptome

Gene ID	FPKM	Annotation	*E* value
Cluster-6061.5327	534484.6	*Bathymodiolus platifrons* mitochondrion, complete genome (NT description)	0
Cluster-6061.5328	524299.8	*Bathymodiolus platifrons* mitochondrion, complete genome (NT description)	0
Cluster-6061.5060	84327.34	Interleukin-4 receptor alpha chain, N-terminal/ATP synthase protein 8 (PFAM Description)	0
Cluster-6061.4508	37132.12	Ribosomal protein L44 [*Azumapecten farreri*] (NR description)	3.60E-52
Cluster-6061.4964	31102.76	Cytochrome c oxidase subunit III (mitochondrion) [*Bathymodiolus platifrons*] (NR description)	2.30E-117
Cluster-6061.5382	29619.84	ATP synthase F0 subunit 6 (mitochondrion) [*Bathymodiolus securiformis*] (NR Description)	5.90E-41
Cluster-6061.5267	24377.93	40S ribosomal protein S12-like [*Crassostrea virginica*] (NR description)	6.50E-65
Cluster-6061.5192	15565.89	40S ribosomal protein S26-like [*Mizuhopecten yessoensis*] (NR description)	1.40E-34
Cluster-6061.5163	14261.83	Cytochrome c oxidase subunit I (mitochondrion) [*Bathymodiolus securiformis*] (NR description)	6.20E-263
Cluster-6061.5429	13021.48	ATP synthase F0 subunit 6 (mitochondrion) [*Bathymodiolus platifrons*] (NR Description)	6.50E-93
Cluster-6061.5644	12286.37	Ribosomal protein [*Pinctada fucata*] (NR description)	9.00E-59
Cluster-6061.4493	10793.48	Ribosomal protein [*Mytilus galloprovincialis*] (NR description)	1.40E-19
Cluster-6061.5164	10398.21	NADH dehydrogenase subunit 1 (mitochondrion) [*Bathymodiolus platifrons*] (NR description)	1.10E-154
Cluster-6061.5591	9563.027	NADH dehydrogenase subunit 4 (mitochondrion) [*Bathymodiolus platifrons*] (NR description)	1.70E-165
Cluster-6061.4156	8762.687	PREDICTED: 40S ribosomal protein S19-like [*Octopus bimaculoides*] (NR Description)	3.50E-58
Cluster-6061.5127	8348.013	Ribosomal protein [*Mytilus trossulus*] (NR description)	5.70E-23
Cluster-6061.5519	7945.677	40S ribosomal protein S20 [*Crassostrea virginica*] (NR description)	7.10E-56
Cluster-6061.4653	7866.61	PREDICTED: 60S ribosomal protein L37a [*Crassostrea gigas*] (NR description)	5.10E-40
Cluster-6061.5134	7825.263	NADH dehydrogenase subunit 6 (mitochondrion) [*Bathymodiolus platifrons*] (NR description)	1.80E-29
Cluster-6061.5019	7821.213	60S ribosomal protein L35-like [*Crassostrea virginica*] (NR description)	2.40E-50

3.4 Tissue Expression of Genes Related to Biomineralisation

All the transcriptome data were searched and 11 SMPs were detected in the foot, gill, muscle, and mantle tissues *via* qPCR (Fig.5). Five genes (*nacrein*, *perlucin*, *perlwapin*, *pif* and *mantle protein*) were significantly expressed in mantle tissue, five genes (*chitinase*, *ferritin*, *SPARC-related modular calcium-binding protein 1-like isoform X2* (*SPARC*), *tyrosinase-like protein* (*TRY*), *papilin* and *calmodulin*) were expressed lowly in mantle tissue, and only *perlucin* was exclusively expressed in mantle tissue.

3.5 SEM Images of the *G. haimaensis* Shell

The structure of the shell was observed using SEM. It was composed of an outermost prismatic layer with a nacreous layer beneath (Figs.6a−d). The nacreous layer has a multilayer structure, and is made of whole pieces of aragonite that stack on top of each other, but not with quadrilateral or polygonal pieces of nacreous layers connected to each other (Figs.6c, d), as described previously by Shi *et al*. (2020).

4 Discussion

Mitochondria are the only organelles containing extranuclear DNA (mtDNA) in humans and other animals. Mitochondria are the main site of aerobic metabolism, and generate ATP through a series of oxidative phosphorylation processes, providing more than 90% of the body's energy supply (Lee and Wei, 2000). The function of mtDNA is not only related to its structural integrity, but also its copy number; an increase in copy number is believed to support mitochondrial respiratory function (Lee and Wei, 2000). Therefore, as the power stations of cells, mitochondria play a crucial role in cell damage caused by hypoxia, and the adaptation of tissues and cells to a hypoxic environment (Agani *et al*., 2000). In the process of environmental adaptation, mitochondrial morphology, function, and mtDNA sequence can all change (Zhang *et al*., 1997). Studies on the functions of mtDNA on environmental fitness have mainly focused on the bird *Tetraogallus himalayensis* in East Pamir (An *et al*., 2016), the Eastern honey bee *Apis cerana* on the Qinghai-Tibet Plateau (Yu *et al*., 2019), and pika (Li *et al*., 2018). Studies on the adaptability of species in a deep-sea high-pressure anoxic environment are scarce. Analysis of the top 20 most highly expressed genes in transcriptomes revealed that expression levels of mitochondrial genes are extremely high, and genes related to energy supply such as *cytochrome c oxidase*, *NADH dehydrogenase* and *ATP synthase F0* are typically in the top 20 most high-

ly expressed genes. For example, high expressions of *cytochrome c oxidase* and *NADH dehydrogenase* were reported among the top 20 most highly expressed genes in the shallow-sea mollusc *Pinctada fucata martensii*, but no mi-

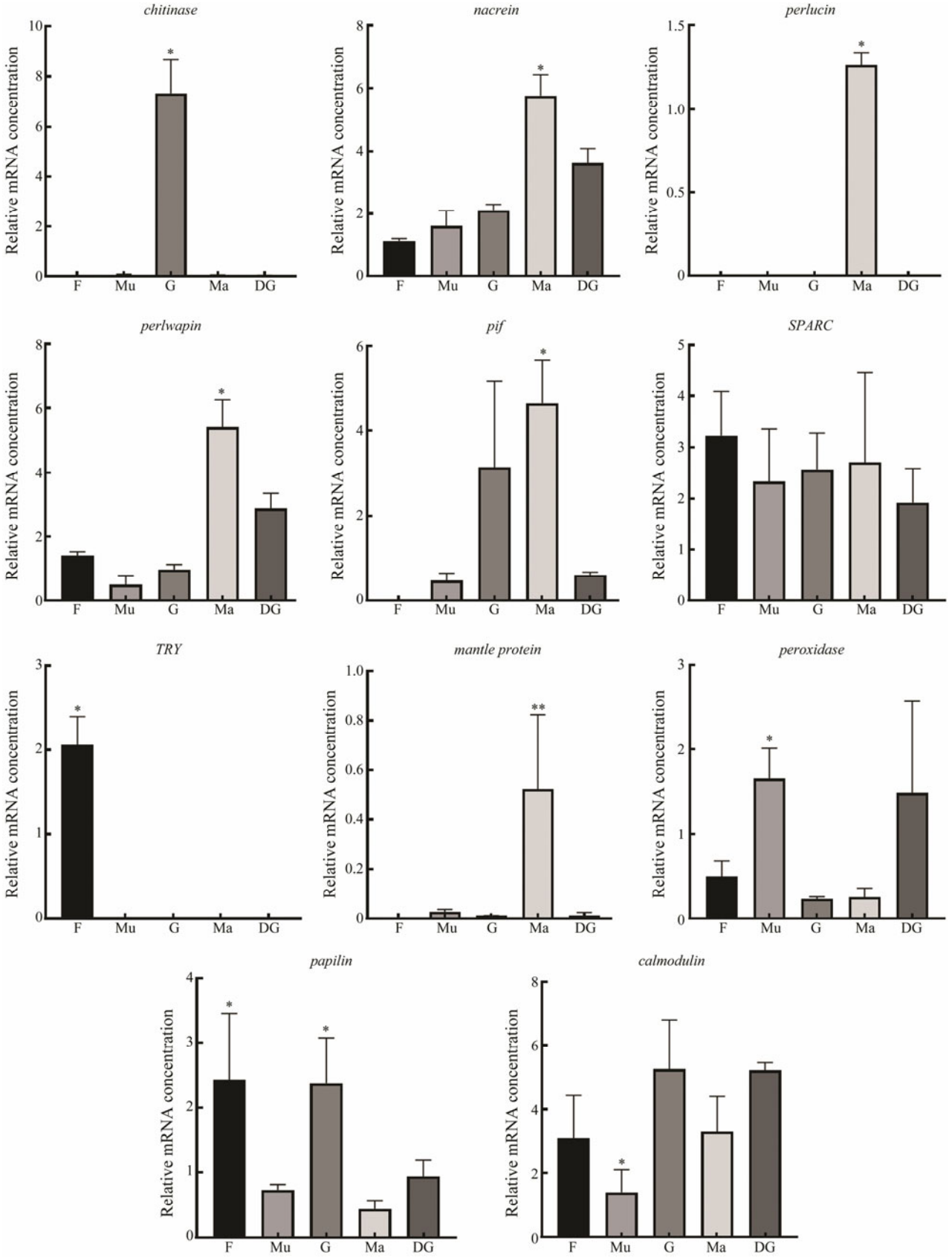

Fig.5 Expression levels of eleven SMP genes examined in the foot (F), muscle (M), gill (G), mantle (Ma) and digestive gland (DG) of *G. haimaensis* obtained *via* qPCR. Results are shown as mean±standard deviation (S.D.) of samples ($n=3$) and are expressed as fold-change in mRNA expressions. Significant differences are indicated by an asterisk (* $P<0.05$). *SPARC*, SPARC-related modular calcium-binding protein 1-like isoform X2; *TRY*, tyrosinase-like protein 1.

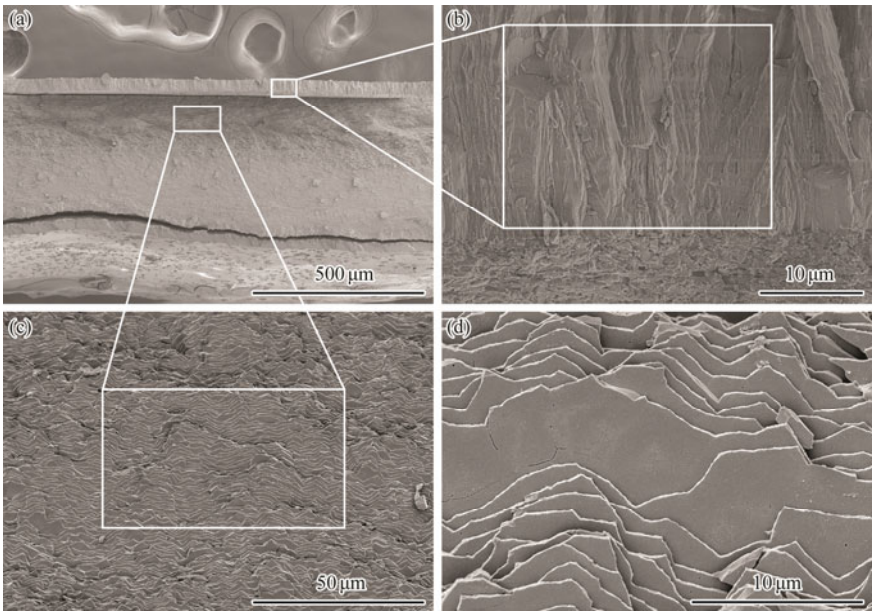

Fig.6 SEM images of *G. haimaensis*'s shell. (a), Panoramic view of horizontal images of the shell. Scale bar = 500 μm; (b), Horizontal image of the prismatic layer. Scale bar = 10 μm. (c) and (d), Horizontal images of the nacreous layer. Scale bar = 50 μm (c) and 10 μm (d).

tochondrial genes were identified (Xu *et al*., 2019a). These results suggest that the increase of mitochondrial gene copy numbers may be related to the adaptability of deep-sea mussels to the high-pressure hypoxic environment, and the increase in mitochondrial gene, cytochrome c oxidase, NADH dehydrogenase and ATP synthase F0 copy numbers may strengthen respiratory function.

Chitin is a major component of mollusc shell organic matter. The framework growth model (Addadi *et al*., 2006) predicts that before mineral deposition, the insoluble organic matrix framework is first formed by chitin, and chitin in the framework is arranged in a highly ordered manner. Calcium carbonate crystals then nucleate and grow at specific parts on the organic framework. Chitinase plays a crucial role in chitin metabolism, hence it may be participating in the formation of the shell organic framework.

Among all enzymes involved in the physiological processes of chitin, chitin synthase (CS) (Behr *et al*., 2001) and chitinase play the most prominent roles. Chitin synthase is a membrane-bound glycoside invertase, which can synthesise chitin precursors into chitin and promote the elongation of chitin molecules. Conversely, chitinase catalyses the hydrolysis of chitin. The two functions complement each other to control the synthesis and hydrolysis of chitin, and thereby regulate chitin physiological processes.

The only framework protein-related *chitinase* found in mussels was not highly expressed in mantle in the present work, possibly because there are many types of *chitinase*, and the examined *chitinase* was not involved in biomineralisation. It is also possible that as mussels mature, the growth of shells slows or stalls, and expression of *chitinase* may be inhibited.

We identified five acidic and nacreous SMPs (*nacrein*, *perlucin*, *perlwapin*, *pif* and *mantle protein*) expressed at high levels in mantle in *G. haimaensis*.

Nacrein was the first SMP identified in *P. fucata martensii*, which was shown to mainly regulate the nacre formation (Miyamoto *et al*., 2005). Subsequent studies found that it is also present in the prismatic layer of the shell (Treccani *et al*., 2006), hence it may regulate the mineralization of both nacre and prismatic layers of the whole shell. Nacrein protein has two functional domains; a gly-x-asn domain (x is Asp, Asn or Glu) that bonds calcium ions, and a carbonic anhydrase domain that catalyses the formation of $HCO3^{-}$ ions. The results of crystallisation experiments *in vitro* showed that the gly-x-asn repeat region could inhibit the precipitation of calcium carbonate, indicating that Nacrein may play a negative role in shell calcification (Miyamoto *et al*., 1996; Miyamoto *et al*., 2005).

Perlucin was first SMP separated from the nacre of Abalone, regulating the formation of pearl and shell by increasing the precipitation of calcium carbonate, connecting aragonite and chitin layers, and promoting growth of calcium carbonate crystals and the nucleation (Weiss *et al*., 2000).

Perlwapin is a growth inhibitor of calcium carbonate crystals in saturated calcium carbonate solution. It may inhibit the growth of some crystal planes in the mineral phase of nacre in polymer/mineral composites in the growth of nacre (Treccani *et al*., 2006).

Strong expressions of *nacrein*, *perlucin*, *perlwapin* and *mantle protein* in mantle tissue indicate their roles in biomineralisation in *G. haimaensis*. Furthermore, shell scanning results suggest that *nacrein* may be mainly involved in the formation of the nacreous layer rather than the prismatic layer in *G. haimaensis*.

The formation of mineral precursors usually involves amorphous calcium carbonate (ACC). ACC is considered to be the precursor of biominerals and is abundant in various organisms (Nassif *et al*., 2005). To form ACC, molluscs need high concentrations of CO_3^{2-} and Ca^{2+} in seawa-

ter. Ca^{2+} can be concentrated by acidic proteins such as Pif (Suzuki *et al*., 2009) and Aspein (Takeuchi *et al*., 2008), while CO_3^{2-} can be concentrated by carbonic anhydrase enzymes such as nacrein. Pif has a chitin-binding domain that binds chitin and participates in controlling the formation of mineral precursors (Bahn *et al*., 2015). *In vivo*, Pif may work together with N16 protein to regulate the morphology of aragonite fragments by controlling its growth and the crystallisation in nacre, which plays a pivotal role in the normal deposition and development of nacre (Suzuki *et al*., 2009). Pif plays multiple functions in different stages of biomineralisation, and high expression of *pif* in mantle tissue suggests a role in biomineralisation in *G. haimaensis*. It may also play a crucial role in crystal growth by binding to calcium carbonate.

SPARC is a matricellular protein which might play a role in bone formation and mineralisation in vertebrates and invertebrates (Choi *et al*., 2010). Papilin is also found among nacre matrix proteins in *Elliptio complanate* and *Villosa lienosa* (Marie *et al*., 2017). The main function of calmodulin is transport and absorption of calcium ions (Li *et al*., 2004), suggesting a role in biomineralisation. Herein, *SPARC*, *papilin* and *calmodulin* were expressed in all tissues in *G. haimaensis*, not only in mantle, implying diverse functions of *SPARC* and *papilin* in addition to biomineralisation in mantle.

Tyrosinase-like protein, an acidic SMP, is usually in charge of the production of melanin in the prismatic layer (Jimbow, 1999). Overall expression levels of *try* were very low in this deep-sea mussel, but relatively high in the foot, implying that it may not be involved in the generation of melanin in the prismatic layer.

5 Conclusions

In summary, we report a comprehensive transcript dataset obtained from the mantle tissue of the deep-sea mussel *G. haimaensis* using an Illumina Novaseq platform. A total of 30255 unigenes were assembled from 21036211 filtered clean reads. The data provide a common genomic resource for understanding the characteristics of deep-sea mussel biomineralisation. The top 20 most highly expressed genes were annotated as genes related to energy supply, including mitochondrial genes, suggesting they may be related to the adaptability of deep-sea mussels to the high-pressure and hypoxic environment. Eleven SMP-related genes were identified from the transcriptome data, and qPCR results showed that five of ten acidic SMPs plus nacreous matrix genes (*nacrein*, *perlucin*, *perlwapin*, *pif* and *mantle protein*) were significantly expressed in mantle tissue, while five genes (*chitinase*, *SPARC*, *TRY*, *papilin* and *calmodulin*) were expressed lowly in mantle tissue. SEM results showed that the shell is composed of a prismatic layer with a nacreous layer beneath, and the nacreous layer is made of whole pieces of aragonite that stacks on top of each other. These results indicate that the structures and functions of nacreous matrix proteins are conserved in *G. haimaensis*, and the nacreous layer is built from whole pieces of aragonite, not from quadrilateral or polygonal pieces. The identified genes will contribute to studies on the molecular mechanisms of biomineralisation in *G. haimaensis*, and provide a new perspective for studying biomineralisation mechanisms in other deep-sea mussels.

Acknowledgements

This project was supported by the Key Special Project for Introduced Talents Team of Southern Marine Science and Engineering Guangdong Laboratory, Guangzhou, China (No. GML2019ZD0401), the Major Project of Basic and Applied Basic Research of Guangdong Province (No. 2019 B030302004), and the Science and Technology Planning Project of Guangdong Province, China (No. 2020B12120 60058). We would like to thank Dr. Chen for providing photos of *G. haimaensis*.

References

Abe, K., Iwamoto, S., and Yano, H., 2007. Obtaining cellulose nanofibers with a uniform width of 15 nm from wood. *Biomacromolecules*, **8**: 3276-3278, DOI: 10.1021/bm700624p.

Addadi, L., Joester, D., Nudelman, F., and Weiner, S., 2006. Mollusk shell formation: A source of new concepts for understanding biomineralization processes. *Chemistry*, **12**: 980-987, DOI: 10.1002/chem.200500980.

Agani, F. H., Pichiule, P., Chavez, J. C., and Lamanna, J. C., 2000. The role of mitochondria in the regulation of hypoxia-inducible factor 1 expression during hypoxia. *Journal of Biological Chemistry*, **275**: 35863-35867, DOI: 10.1074/jbc.M005643200.

An, B., Zhang, L. X., Ruan, L. Z., Liu, N. F., Zhang, Z. X., Abutalip, A., *et al*., 2016. The complete mitochondrial genome of Himalayan snowcock (*Tetraogallus himalayensis*). *Mitochondrial DNA Part A*, **27**: 3751-3752, DOI: 10.3109/19401736.2015.1079889.

Artigaud, S., Thorne, M. A., Richard, J., Lavaud, R., Jean, F., Flye-Sainte-Marie, J., *et al*., 2014. Deep sequencing of the mantle transcriptome of the great scallop *Pecten maximus*. *Marine Genomics*, **15**: 3-4, DOI: 10.1016/j.margen.2014.03.006.

Bahn, S. Y., Jo, B. H., Hwang, B. H., Choi, Y. S., and Cha, H. J., 2015. Role of Pif97 in nacre biomineralization: *In vitro* characterization of recombinant Pif97 as a framework protein for the association of organic-inorganic layers in nacre. *Crystal Growth & Design*, **15**: 3666-3673, DOI: 10.1021/acs.cgd.5b00275.

Behr, J. B., Gautier-Lefebvre, I., Mvondo-Evina, C., Guillerm, G., and Ryder, N. S., 2001. Inhibition of chitin synthetase from *Saccharomyces cerevisiae* by a new UDP-GlcNAc analogue. *Journal of Enzyme Inhibition and Medicinal Chemistry*, **16**: 107-112, DOI: 10.1080/14756360109162360.

Bettencourt, R., Pinheiro, M., Egas, C., Gomes, P., Afonso, M., Shank, T., *et al*., 2010. High-throughput sequencing and analysis of the gill tissue transcriptome from the deep-sea hydrothermal vent mussel *Bathymodiolus azoricus*. *BMC Genomics*, **11**: 559, DOI: 10.1186/1471-2164-11-559.

Bougerol, M., Boutet, I., Leguen, D., Jollivet, D., and Tanguy, A., 2015. Transcriptomic response of the hydrothermal mussel *Bathymodiolus azoricus* in experimental exposure to heavy metals is modulated by the Pgm genotype and symbiont content. *Marine Genomics*, **21**: 63-73, DOI: 10.1016/j.margen.2014.11.010.

Boutet, I., Jollivet, D., Shillito, B., Moraga, D., and Tanguy, A., 2009. Molecular identification of differentially regulated genes

in the hydrothermal-vent species *Bathymodiolus thermophilus* and *Paralvinella pandorae* in response to temperature. *BMC Genomics*, **10**: 222, DOI: 10.1186/1471-2164-10-222.

Campbell, K. A., 2000. The ecology of deep-sea hydrothermal vents. *Science*, **289**: 730-731.

Choi, Y. A., Lim, J., Kim, K. M., Acharya, B., Cho, J. Y., Bae, Y. C., *et al*., 2010. Secretome Analysis of human BMSCs and identification of SMOC1 as an important ECM Protein in osteoblast differentiation. *Journal of Proteome Research*, **9**: 2946-2956, DOI: 10.1021/pr901110q.

Deng, Y. W., Lei, Q. N., Tian, Q. L., Xie, S. H., Du, X. D., Li, J. H., *et al*., 2014. De novo assembly, gene annotation, and simple sequence repeat marker development using Illumina paired-end transcriptome sequences in the pearl oyster *Pinctada maxima*. *Bioscience Biotechnology and Biochemistry*, **78**: 1685-1692, DOI: 10.1080/09168451.2014.936351.

Dubilier, N., Bergin, C., and Lott, C., 2008. Symbiotic diversity in marine animals: The art of harnessing chemosynthesis. *Nature Reviews Microbiology*, **6**: 725-740, DOI: 10.1038/nrmicro1992.

Dujardin, E., and Mann, S., 2002. Bio-inspired materials chemistry. *Advanced Engineering Materials*, **4**: 461-474, DOI: 10.1002/1527-2648(20020717)4:7<461::AID-ADEM461>3.0.CO;2-K.

Freer, A., Bridgett, S., Jiang, J., and Cusack, M., 2014. Biomineral proteins from *Mytilus edulis* mantle tissue transcriptome. *Marine Biotechnology (NY)*, **16**: 34-45, DOI: 10.1007/s10126-013-9516-1.

Hasegawa, Y., and Uchiyama, K., 2005. cDNA clonings of shell matrix proteins from scallop shell. *Fisheries Science*, **71**: 1174-1178, DOI: 10.1111/j.1444-2906.2005.01078.x.

Heuer, A. H., and Fink, D. J., 1992. Innovative materials processing strategies: A biomimetic approach. *Science*, **255**: 1098-1105, DOI: 10.1126/science.1546311.

Huang, J., Zhang, C., Ma, Z., Xie, L., and Zhang, R., 2007. A novel extracellular EF-hand protein involved in the shell formation of pearl oyster. *Acta Biochimica and Biophysica Sinica (Shanghai)*, **1770**: 1037-1044, DOI: 10.1016/j.bbagen.2007.03.006.

Huang, Z. M., Zhang, Y. Z., Kotaki, M., and Ramakrishna, S., 2003. A review on polymer nanofibers by electrospinning and their applications in nanocomposites. *Composites Science and Technology*, **63**: 2223-2253, DOI: 10.1016/S0266-3538(03)00178-7.

Isowa, Y., Sarashina, I., Oshima, K., Kito, K., Hattori, M., and Endo, K., 2015. Proteome analysis of shell matrix proteins in the brachiopod *Laqueus rubellus*. *Proteome Science*, **13**: 21, DOI: 10.1186/s12953-015-0077-2.

Jimbow, K., 1999. Biological role of tyrosinase-related protein and its relevance to pigmentary disorders (*Vitiligo vulgaris*). *Journal of Dermatological*, **2**: 734-737, DOI: 10.1111/j.1346-8138.1999.tb02084.x.

Johnson, S. B., Won, Y. J., Harvey, J. B. J., and Vrijenhoek, R. C., 2013. A hybrid zone between *Bathymodiolus* mussel lineages from eastern Pacific hydrothermal vents. *BMC Evolutionary Biology*, **13**: 21, DOI: 10.1186/1471-2148-13-21.

Kong, J. J., Liu, C., Yang, D., Yan, Y., Chen, Y., Liu, Y. J., *et al*., 2019. A novel basic matrix protein of *Pinctada fucata*, PNU9, functions as inhibitor during crystallization of aragonite. *Crystengcomm*, **21**: 1250-1261, DOI: 10.1039/C8CE02194E.

Kong, Y. W., Jing, G., Yan, Z. G., Li, C. Z., and Gong, N. P., 2009. Cloning and characterization of Prisilkin-39, a novel matrix protein serving a dual role in the prismatic layer formation from the oyster *Pinctada fucata*. *Journal of Biological Chemistry*, **284**: 10841-10854, DOI: 10.1074/jbc.M808357200.

Lee, H. C., and Wei, Y. H., 2000. Mitochondrial role in life and death of the cell. *Journal of Biomedical Science*, **7**: 2-15, DOI: 10.1007/BF02255913.

Levin, L. A., 2005. Ecology of cold seep sediments: Interactions of fauna with flow, chemistry and microbes. *Oceanography and Marine Biology−An Annual Review*, **43**: 1-46, DOI: 10.1201/9781420037449.ch1.

Li, J., Bai, Z. Z., and Ge, R. L., 2018. The expression and significance of PTEN, CPT1A and COX4 in lipid metabolism related tissues of plateau pika. *High Altitude Medicine & Biology*, **39**: 79-82.

Li, S., Xie, L., Zhang, C., Zhang, Y., Gu, M., and Zhang, R., 2004. Cloning and expression of a pivotal calcium metabolism regulator: Calmodulin involved in shell formation from pearl oyster (*Pinctada fucata*). *Comparative Biochemistry & Physiology Part B: Biochemistry & Molecular Biology*, **138**: 235-243, DOI: 10.1016/j.cbpc.2004.03.012.

Liu, H. L., Liu, S. F., Ge, Y. J., Liu, J., Wang, X. Y., Xie, L. P., *et al*., 2007. Identification and characterization of a biomineralization related gene PFMG1 highly expressed in the mantle of *Pinctada fucata*. *Biochemistry*, **46**: 844-851, DOI: 10.1021/bi061881a.

Ma, Z., Huang, J., Sun, J., Wang, G., Li, C., and Zhang, R., 2007. A novel extrapallial fluid protein controls the morphology of nacre lamellae in the pearl oyster, *Pinctada fucata*. *Journal of Biological Chemistry*, **282**: 23253-23263, DOI: 10.1074/jbc.M700001200.

Mao, X. Z., Cai, T., Olyarchuk, J. G., and Wei, L. P., 2005. Automated genome annotation and pathway identification using the KEGG Orthology (KO) as a controlled vocabulary. *Bioinformatics*, **21**: 3787-3793, DOI: 10.1093/bioinformatics/bti430.

Marie, B., Arivalagan, J., Matheron, L., Bolbach, G., Gerard, B., Sophie, M., *et al*., 2017. Deep conservation of bivalve nacre proteins highlighted by shell matrix proteomics of the *Unionoida Elliptio complanata* and *Villosa lienosa*. *Journal of the Royal Society Interface*, **14** (126): 20160846, DOI: 10.1098/rsif.2016.0846.

Marie, B., Joubert, C., Tayale, A., Belliard, P., Cochennec-Laureau, M., and Gueguen, M., 2012. Different secretory repertoires control the biomineralization processes of prism and nacre deposition of the pearl oyster shell. *Proceedings of the National Academy of Sciences of the United States of America*, **109**: 20986-20991, DOI: 10.1073/pnas.1210552109.

Mariom, Take, S., Igarashi, Y., Yoshitake, K., Asakawa, S., Maeyama, K., *et al*., 2019. Gene expression profiles at different stages for formation of pearl sac and pearl in the pearl oyster *Pinctada fucata*. *BMC Genomics*, **20** (1): 240, DOI: 10.1186/s12864-019-5579-3.

Masaoka, T., and Kobayashi, T., 2009. Analysis of nucleotide variation and inheritance of lysine-rich matrix protein (KRMP) genes participating in shell formation of pearl oyster. *DNA Polymorphism*, **17**: 126-135.

Miyamoto, H., Endo, H., Hashimoto, N., Limura, K., Isowa, Y., Kinoshita, S., *et al*., 2013. The diversity of shell matrix proteins: Genome-wide investigation of the pearl oyster, *Pinctada fucata*. *Zoological Science*, **30** (10): 801-816, DOI: 10.2108/zsj.30.801.

Miyamoto, H., Miyashita, T., Okushima, M., Nakano, S., Morita, T., and Matsushiro, A., 1996. A carbonic anhydrase from the nacreous layer in oyster pearls. *Proceedings of the National Academy of Sciences of the United States of America*, **93**: 9657-9660, DOI: 10.1073/pnas.93.18.9657.

Miyamoto, H., Miyoshi, F., and Kohno, J., 2005. The carbonic anhydrase domain protein nacrein is expressed in the epithelial cells of the mantle and acts as a negative regulator in calcifi-

cation in the mollusc *Pinctada fucata*. *Zoological Science*, **22**: 311-315, DOI: 10.2108/zsj.22.311.

Miyashita, T., Takagi, R., Okushima, M., Nakano, S., Miyamoto, H., Nishikawa, E., *et al*., 2000. Complementary DNA cloning and characterization of pearlin, a new class of matrix protein in the nacreous layer of oyster pearls. *Marine Biotechnology (NY)*, **2**: 409-418, DOI: 10.1007/s101260000013.

Nassif, N., Pinna, N., Gehrke, N., Antonietti, M., Jager, C., and Colfen, H., 2005. Amorphous layer around aragonite platelets in nacre. *Proceedings of the National Academy of Sciences of the United States of America*, **102**: 12653-12655, DOI: 10.1073/pnas.0502577102.

Pan, C., Fang, D., Xu, G., Liang, J., Zhang, G., Wang, H., *et al*., 2014. A novel acidic matrix protein, PfN44, stabilizes magnesium calcite to inhibit the crystallization of aragonite. *Journal of Biological Chemistry*, **289**: 2776-2787, DOI: 10.1074/jbc.M113.504027.

Ren, D., Feng, Q., and Bourrat, X., 2011. Effects of additives and templates on calcium carbonate mineralization *in vitro*. *Micron*, **42**: 228-245, DOI: 10.1016/j.micron.2010.09.005.

Sarashina, I., and Endo, K., 2001. The complete primary structure of molluscan shell protein 1 (MSP-1), an acidic glycoprotein in the shell matrix of the scallop *Patinopecten yessoensis*. *Marine Biotechnology*, **3**: 362-369, DOI: 10.1007/s10126-001-0013-6.

Semeao, E. J., Jawad, A. F., Zemel, B. S., Neiswender, K. M., Piccoli, D. A., and Stallings, V. A., 1999. Bone mineral density in children and young adults with Crohn's disease. *Inflammatory Bowel Disease*, **5**: 161-166, DOI: 10.1097/00054725-199908000-00003.

Shi, M., Lin, Y., Xu, G., Xie, L. P., Hu, X. L., Bao, Z. M., *et al*., 2013a. Characterization of the Zhikong scallop (*Chlamys farreri*) mantle transcriptome and identification of biomineralization-related genes. *Marine Biotechnology (NY)*, **15**: 706-715, DOI: 10.1007/s10126-013-9517-0.

Shi, Y., Yao, G., Zhang, H., Jia, H., Xiong, P., and He, M., 2022. Proteome and transcriptome analysis of gonads reveals intersex in *Gigantidas haimaensis*. *BMC Genomics*, **23**: 174, DOI: 10.1186/s12864-022-08407-w.

Shi, Y., Yu, C., Gu, Z., Zhan, X., Wang, Y., and Wang, A., 2013b. Characterization of the pearl oyster (*Pinctada martensii*) mantle transcriptome unravels biomineralization genes. *Marine Biotechnology (NY)*, **15**: 175-187, DOI: 10.1007/s10126-012-9476-x.

Shi, Y., Zhao, M., and He, M. X., 2020. PfSMAD1/5 can interact with PfSMAD4 to inhibit PfMSX to regulate shell biomineralization in *Pinctada fucata martensii*. *Marine Biotechnology*, **22**: 246-262, DOI: 10.1007/s10126-020-09948-5.

Sibuet, M., and Olu, K., 1998. Biogeography, biodiversity and fluid dependence of deep-sea cold-seep communities at active and passive margins. *Deep-Sea Research Part I–Topical Studies in Oceanography*, **45**: 517-567, DOI: 10.1016/S0967-0645(97)00074-X.

Sudo, S., Fujikawa, T., Nagakura, T., Ohkubo, T., Sakaguchi, K., Tanaka, M., *et al*., 1997. Structures of mollusc shell framework proteins. *Nature*, **387**: 563-564, DOI: 10.1038/42391.

Sun, J., Chen, C., Miyamoto, N., Li, R. S., Sigwart, J. D., Xu, T., *et al*., 2020. The Scaly-foot Snail genome and implications for the origins of biomineralised armour. *Nature Communication*, **11**: 1657, DOI: 10.1038/s41467-020-15522-3.

Sun, J., Zhang, Y., Xu, T., Zhang, Y., Mu, H. W., Zhang, Y. J., *et al*., 2017. Adaptation to deep-sea chemosynthetic environments as revealed by mussel genomes. *Nature Ecology & Evolution*, **1**: 121, DOI: 10.1038/s41559-017-0121.

Suzuki, M., Murayama, E., Inoue, H., Ozaki, N., Tohse, H., Kogure, T., *et al*., 2004. Characterization of Prismalin-14, a novel matrix protein from the prismatic layer of the Japanese pearl oyster (*Pinctada fucata*). *Biochemical Journal*, **382**: 205-213, DOI: 10.1042/BJ20040319.

Suzuki, M., Saruwatari, K., Kogure, T., Yamomoto, Y., Nishiura, T., Kato, T., *et al*., 2009. An acidic matrix protein, Pif, is a key macromolecule for nacre formation. *Science*, **325**: 1388-1390, DOI: 10.1126/science.1173793.

Takeuchi, T., Sarashina, I., Iijima, M., and Endo, K., 2008. *In vitro* regulation of $CaCO_3$ crystal polymorphism by the highly acidic molluscan shell protein Aspein. *FEBS Letters*, **582**: 591-596, DOI: 10.1016/j.febslet.2008.01.026.

Treccani, L., Mann, K., Heinemann, F., and Fritz, M., 2006. Perlwapin, an abalone nacre protein with three four-disulfide core (whey acidic protein) domains, inhibits the growth of calcium carbonate crystals. *Biophysical Journal*, **91**: 2601-2608, DOI: 10.1529/biophysj.106.086108.

Wang, N., Kinoshita, S., Riho, C., Maeyama, K., Nagai, K., and Watabe, S., 2009. Quantitative expression analysis of nacreous shell matrix protein genes in the process of pearl biogenesis. *Comparative Biochemistry & Physiology Part B: Biochemistry & Molecular Biology*, **154**: 346-350, DOI: 10.1016/j.cbpb.2009.07.012.

Weiss, I. M., Kaufmann, S., Mann, K., and Fritz, M., 2000. Purification and characterization of perlucin and perlustrin, two new proteins from the shell of the mollusc *Haliotis laevigata*. *Biochemical and Biophysical Research Communication*, **267**: 17-21, DOI: 10.1006/bbrc.1999.1907.

Werner, G. D., Gemmell, P., Grosser, S., Hamer, R., and Shimeld, S. M., 2013. Analysis of a deep transcriptome from the mantle tissue of *Patella vulgata* Linnaeus (Mollusca: Gastropoda: Patellidae) reveals candidate biomineralising genes. *Marine Biotechnology (NY)*, **15**: 230-243, DOI: 10.1007/s10126-012-9481-0.

Xu, M., Huang, J., Shi, Y., Zhang, H., and He, M., 2019a. Comparative transcriptomic and proteomic analysis of yellow shell and black shell pearl oysters, *Pinctada fucata martensii*. *BMC Genomics*, **20**: 469, DOI: 10.1186/s12864-019-5807-x.

Xu, T., Feng, D., Tao, J., and Qiu, J. W., 2019b. A new species of deep-sea mussel (Bivalvia: Mytilidae: *Gigantidas*) from the South China Sea: Morphology, phylogenetic position, and gill-associated microbes. *Deep-Sea Research Part I–Oceanographic Research Papers*, **146**: 79-90, DOI: 10.1016/j.dsr.2019.03.001.

Yano, M., Nagai, K., Morimoto, K., and Miyamoto, H., 2006. Shematrin: A family of glycine-rich structural proteins in the shell of the pearl oyster *Pinctada fucata*. *Comparative Biochemistry and Physiology Part B: Biochemistry & Molecular Biology*, **144**: 254-262, DOI: 10.1016/j.cbpb.2006.03.004.

Young, M. D., Wakefield, M. J., Smyth, G. K., and Oshlack, A., 2010. Gene ontology analysis for RNA-seq: Accounting for selection bias. *Genome Biology*, **11**: R14, DOI: 10.1186/gb-2010-11-2-r14.

Yu, Y., Zhou, S., Zhu, X., Xu, X. J., Wang, W. F., Zha, L., *et al*., 2019. Genetic differentiation of eastern honey bee (*Apis cerana*) populations across Qinghai-Tibet Plateau-valley landforms. *Frontiers in Genetics*, **10**: 483, DOI: 10.3389/fgene.2019.00483.

Zhang, X. M., Yang, Y., Wang, B. Z., Zhang, D. T., Yu, M., and Chen, D. H., 1997. Structural and functional changes of mitochondria in myocardial cells from heart failure in plateau. *Chinese Science Bulletin*, **42**: 76-79, DOI: 10.1007/BF02882528.

Zhang, Y., Xie, L., Meng, Q., Jiang, T. M., and Zhang, R. Q., 2003. A novel matrix protein participating in the nacre framework formation of pearl oyster, *Pinctada fucata*. *Comparative Biochemistry and Physiology Part B: Biochemistry & Molecular Biology*, **135**: 565-573, DOI: 10.1016/S1096-4959(03)00138-6.

(Edited by Qiu Yantao)